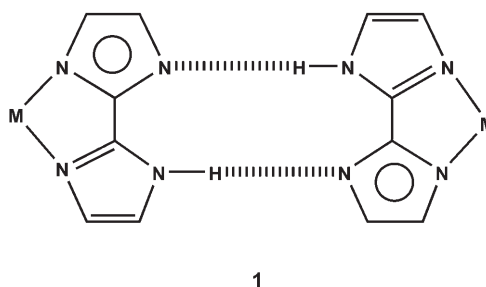


# Mixed-Valence States Stabilized by Proton Transfer in a Hydrogen-Bonded Biimidazolate Rhenium Dimer\*\*

Makoto Tadokoro,\* Tomonori Inoue, Satoru Tamaki, Keisuke Fujii, Kazuo Isogai, Hiroshi Nakazawa, Sadamu Takeda, Kiyoshi Isobe, Nobuaki Koga, Akio Ichimura, and Kazuhiro Nakasuji

Synchronized motion between protons and electrons has already been recognized as a key step in certain biological molecular systems that perform ATP synthesis by using active proton pumps as well as through the conduction of electrons by cytochrome *c* in living matter.<sup>[1]</sup> However, such biological systems are so intrinsically complicated that the driving mechanism is not currently understood completely.<sup>[2]</sup> Therefore, the investigation of molecular materials that exhibit cooperative proton and electron transfer is important for attempts to create new types of artificial materials.<sup>[3]</sup> We have focused on H-bonding dimer complex **1** (M = transition-metal

fragment), which has two metal redox centers and is connected by complementary dual H-bonds. The protons involved in the H-bonds can move easily along a low-barrier double-well potential-energy surface.<sup>[4]</sup> Therefore, the electronic state can be changed from a symmetrical double-well potential into an unsymmetrical one by electrochemical redox reactions of the two metal centers. Consequently, the H-bonding protons would localize into a lower-energy site in the double well. Herein, we report such molecular systems for the Re<sup>III</sup> H-bonding dimer  $[\{\text{Re}^{\text{III}}\text{Cl}_2(\text{PnBu}_3)_2(\text{Hbim})\}_2]$  (**1**), in



which two Re<sup>III</sup> fragments are connected by intermolecular NH...N H-bonds between complementary 2,2'-biimidazolate (Hbim<sup>−</sup>) ligands.

Direct evidence of cooperative proton electron transfer in crystals has not yet been presented.<sup>[5]</sup> On the basis of direct observations, it is believed that quinhydrone crystals generate a neutral semiquinone radical phase under high pressure: the formation of this radical confirms the proton electron transfer.<sup>[6]</sup> Crystals of TCNQ–DABCO,<sup>[7]</sup> a TCNQ–glyoxylate metal complex,<sup>[8]</sup> and TCNQ–benzbiimidazolium<sup>[9]</sup> exhibit an influence on the synchronized motion and fluctuation in the segregated stacking columns of TCNQ (TCNQ = 7,7,8,8-tetracyano-*p*-quinodimethane; DABCO = 1,4-diazabicyclo-[2.2.2]octane). These motions would also be related to cooperative proton electron transfer. In contrast, proton-coupled electron transfer (PCET) in biimidazoline iron complexes in solution has been demonstrated theoretically by Hammes-Schiffer<sup>[10]</sup> and experimentally Mayer and co-workers;<sup>[11]</sup> in this case, PCET was mediated by solvent molecules and occurred through outer-sphere self-exchange reactions. They demonstrated that the transfer rates of electrons and protons are comparable to each other or the electron-transfer rates are slower than those of proton

[\*] Prof. M. Tadokoro, K. Fujii, K. Isogai

Department of Chemistry  
Faculty of Science  
Tokyo University of Science  
Kagurazaka 1-3, Shinjuku-ku, Tokyo 162-8601 (Japan)  
Fax: (+81) 3-5228-8714  
E-mail: tadokoro@rs.kagu.tus.ac.jp

Homepage: <http://www.rs.kagu.tus.ac.jp/tadokoro/>

T. Inoue, S. Tamaki, Prof. H. Nakazawa, Prof. A. Ichimura  
Department of Complex Systems Science  
Graduate School of Information Science  
Osaka City University  
Sugimoto 3-3-138, Sumiyoshi-ku, Osaka 558-8585 (Japan)

Prof. N. Koga  
Department of Chemistry  
Graduate School of Science  
Nagoya University  
Chikusa-ku Nagoya 464-860 (Japan)

Prof. K. Isobe  
Department of Chemistry  
Graduate School of Natural Science and Technology  
Kanazawa University  
Kadoma-cho, Kanazawa, Ishikawa 920-1192 (Japan)

Prof. S. Takeda  
Department of Chemistry  
Graduate School of Science  
Hokkaido University  
Kita-ku, Sapporo 101-0000 (Japan)

Prof. K. Nakasuji  
School of Materials Science  
Fukui University of Technology  
Gakuen 3-6, Fukui 910-8505 (Japan)

[\*\*] This work was supported by a Grant-in-Aid for Scientific Research on Priority Areas (nos. 16041237 and 16038221) and Scientific Research (B) (no. 16350034) from the Ministry of Education, Culture, Science and Technology of Japan.

Supporting information for this article is available on the WWW under <http://www.angewandte.org> or from the author.

transfer, which provides an estimation of the compensation of outer-sphere solvent reorganization for electron transfer. Furthermore, Bond and Haga have pointed out that protons are released from the 2,2'-benzbiimidazolate ligand of Ru or Os complexes in solution as a result of a decrease in its  $pK_a$  value as the central metal ion is electrochemically oxidized.<sup>[12]</sup> These results can be employed in the design of molecular systems that exhibit cooperative proton electron transfer.

A H-bonding donor and acceptor integrated into a conjugated  $\pi$ -electron framework form a strong H-bond (RAHB: resonance-assisted H-bond) in which the protons involved in H-bonding can move easily on the double-well potential-energy surface through a low barrier to proton transfer.<sup>[13]</sup> For example, the H-bonding dimers of certain carboxylic acid derivatives form homogeneous dual H-bonds with double-well potential-energy surfaces.<sup>[14]</sup> Thus, the two H-bonding protons, even in a crystalline solid, exhibit concerted double-proton transfer through a low transfer barrier with alternation of the bonds of the two carboxylic acids on a nearly symmetrical double-well potential-energy surface.<sup>[15]</sup> The self-complementary intermolecular H-bonds between the Hbim<sup>−</sup> ligands of Re complex **1** also form RAHBs, and the complex undergoes concerted double-proton transfer in this state.<sup>[16]</sup> By performing theoretical calculations for a molecular quantum switch, the strength of the dual H-bonding system was determined to be approximately 27 kcal mol<sup>−1</sup>, which is comparable to that of a weak covalent-like bond.<sup>[17]</sup>

Complex **1** was prepared by a literature procedure.<sup>[18]</sup> [(Re<sup>V</sup>=O)Cl<sub>2</sub>(PPh<sub>3</sub>)<sub>2</sub>]Cl and H<sub>2</sub>bim were refluxed in CH<sub>2</sub>Cl<sub>2</sub> with excess PPh<sub>3</sub> to give an intermediate complex [Re<sup>III</sup>Cl<sub>2</sub>(PPh<sub>3</sub>)<sub>2</sub>(H<sub>2</sub>bim)]Cl in high yield. Then, the two PPh<sub>3</sub> ligands in the complex were exchanged with PnBu<sub>3</sub> ligands to prepare the precursor monomer complex [Re<sup>III</sup>Cl<sub>2</sub>(PnBu<sub>3</sub>)<sub>2</sub>(H<sub>2</sub>bim)]Cl (**2**). H-bonding dimer complex **1** was crystallized as single red crystals by adding NH<sub>3</sub> gas to a solution of **2** in MeOH. Figure 1 shows the crystal structure of dimer **1**.<sup>[19]</sup> The crystal does not contain any cocrystallized solvent molecules. Two neutral units of {Re<sup>III</sup>Cl<sub>2</sub>(PnBu<sub>3</sub>)<sub>2</sub>(Hbim)} are connected

by planar intermolecular NH $\cdots$ N H-bonds between the Hbim<sup>−</sup> ligands. The N $\cdots$ N distance (2.771(3) Å) indicates a relatively strong H-bond interaction.<sup>[20]</sup> In fact, the H-bond of **1** is strong even in nonpolar solvents such as toluene, CH<sub>2</sub>Cl<sub>2</sub>, and diethyl ether, because the H-bonding sites are protected by two aliphatic butyl groups of the PnBu<sub>3</sub> ligands, as observed in the crystal (Figure 1).

Protonated monomer **2** and dimer **1** in [D<sub>8</sub>]toluene at 20°C give well-resolved <sup>1</sup>H NMR spectra, despite the Re<sup>III</sup> paramagnetic center with a d<sup>4</sup> electron configuration (Figure 2). In the spectrum (Figure 2a) of **2**, two signals of

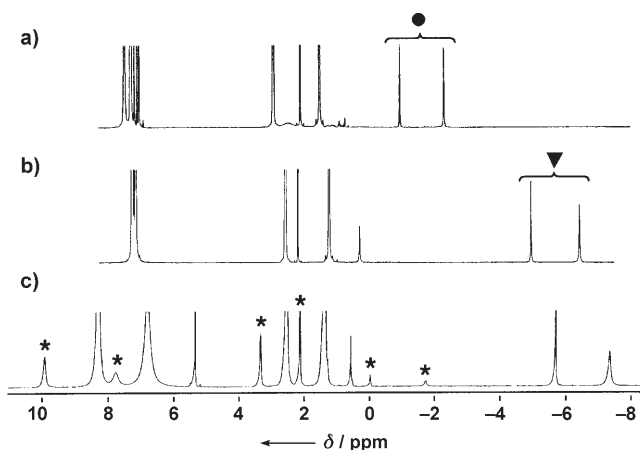


**Figure 2.** <sup>1</sup>H NMR spectra of a) protonated monomer **2** in [D<sub>8</sub>]toluene, b) dimer **1** in [D<sub>8</sub>]toluene at 20°C, and c) **1** in CD<sub>2</sub>Cl<sub>2</sub> at −80°C. Two signals (●) are observed for the aromatic ring protons at the 4- and 5-positions of the Hbim<sup>−</sup> ligand of **2** at  $\delta$  = −2.21 and −0.66 ppm, respectively. These proton signals are shifted in **1** to  $\delta$  = −6.33 and −4.64 ppm (▼). The differences between the signals for the ring protons in **2** and **1** are accounted for by the proximity effect of two paramagnetic Re<sup>III</sup> centers and are an indicator for the H-bonded dimer. The <sup>1</sup>H NMR spectrum of **1** in CD<sub>2</sub>Cl<sub>2</sub> at −80°C (c) shows the existence of a dissociation equilibrium of the dimer to the monomer (whose peaks are indicated by \*).

the aromatic ring protons at the 4- and 5-positions of the Hbim<sup>−</sup> ligand are observed at  $\delta$  = −2.21 and −0.66 ppm, respectively, and a signal for the N–H protons is observed at  $\delta$  = 2.58 ppm. In the spectrum (Figure 2b) of **1**, the H-bonding N–H proton resonates at  $\delta$  = 0.27 ppm and the signals for the 4- and 5-position ring protons occur at  $\delta$  = −6.33 and −4.64 ppm, respectively. These signals and those of the ring in **1** are shifted to higher field by 2.31 ppm and approximately 4 ppm, respectively, relative to the corresponding signals of **2**. These differences are attributed to the proximity effect of the two paramagnetic Re<sup>III</sup> centers. Thus, the signals, which appear at different chemical shifts, can be used to reveal the equilibrium between the monomer and dimer. No obvious dissociation of **1** into the monomer species is observed between −80°C and 70°C in [D<sub>8</sub>]toluene. However, as the temperature rises to 70°C (from −80°C), the two signals of the ring protons are shifted by  $\Delta\delta$  = −0.51 and −1.67 ppm as a result of the exchange between the monomer and dimer at equilibrium. In contrast, the temperature-dependent <sup>1</sup>H NMR spectra of **1** in CD<sub>2</sub>Cl<sub>2</sub> clearly exhibit

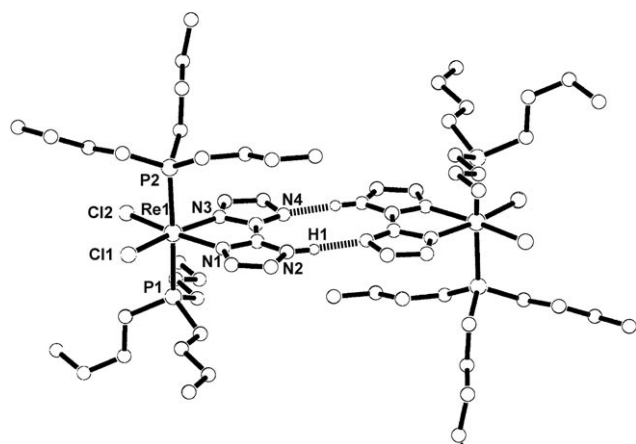


**Figure 1.** A CHARON view of the crystal structure of H-bonded dimer **1**.

dissociation of the dimer. At 20°C, the two ring signals are observed at  $\delta = -6.77$  and  $-4.85$  ppm. However, as the temperature is decreased, two new peaks appear below 0°C at the 4- and 5-positions of the monomer; at  $-80^\circ\text{C}$ , the two signals are observed at  $\delta = -1.75$  and  $-0.04$  ppm for the monomer and  $\delta = -7.36$  and  $-5.69$  ppm for the dimer (Figure 2c). The molar ratio of the monomer and the dimer at  $-80^\circ\text{C}$  is approximately 1:9 for a concentration of  $1.3 \times 10^{-2}$  M (the integration ratio for the dimer/monomer is 9.26 for the 4-position protons and 9.51 for those in the 5-position). Consequently, the dissociation constant  $K$  of **1** in  $\text{CD}_2\text{Cl}_2$  is estimated to be approximately  $1.40 \times 10^{-4}$  M at  $-80^\circ\text{C}$ . This result indicates that the long aliphatic chains of the trialkyl phosphine ligands suppress dissociation.

Cyclic voltammometry (CV) measurements of **1** in  $\text{CH}_2\text{Cl}_2$  reveal characteristic phenomena for cooperative proton electron transfer. Figure 3 shows the cyclic voltam-

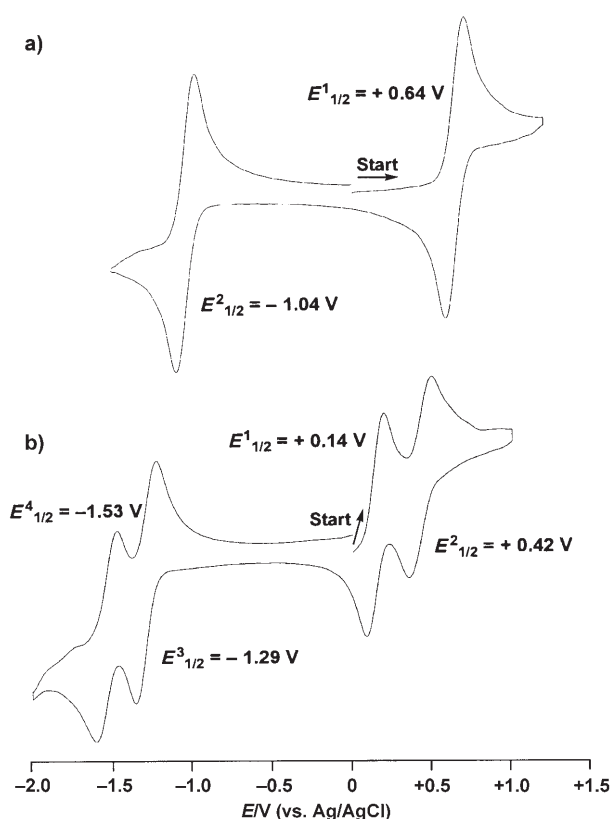
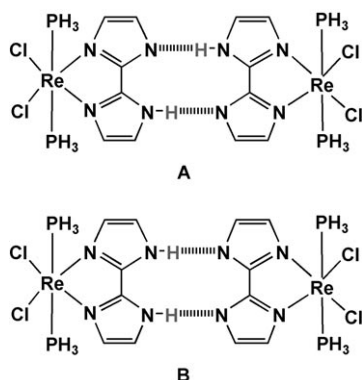


Figure 3. Cyclic voltammograms of a) **2** and b) **1** in  $\text{CH}_2\text{Cl}_2$ .

grams of monomer **2** and dimer **1**. Monomer **2** exhibits two electrochemical redox couples  $\text{Re}^{\text{III}}/\text{Re}^{\text{IV}}$  ( $E_{1/2}^1 = +0.64$  V vs. Ag/AgCl) and  $\text{Re}^{\text{II}}/\text{Re}^{\text{III}}$  ( $E_{1/2}^2 = -1.04$  V vs. Ag/AgCl). In contrast, **1** exhibits four reversible redox couples  $\text{Re}^{\text{III}}/\text{Re}^{\text{IV}}$  ( $E_{1/2}^1 = +0.14$  V vs. Ag/AgCl),  $\text{Re}^{\text{III}}/\text{Re}^{\text{IV}}$  ( $E_{1/2}^2 = +0.42$  V vs. Ag/AgCl),  $\text{Re}^{\text{II}}/\text{Re}^{\text{III}}$  ( $E_{1/2}^3 = -1.29$  V vs. Ag/AgCl), and  $\text{Re}^{\text{II}}/\text{Re}^{\text{III}}$  ( $E_{1/2}^4 = -1.53$  V vs. Ag/AgCl). Interestingly, **1** forms two mixed-valence states  $\text{Re}^{\text{III}}\text{Re}^{\text{IV}}$  and  $\text{Re}^{\text{II}}\text{Re}^{\text{III}}$  over potential ranges of 0.28 V ( $\Delta E_{1/2}^1 = E_{1/2}^2 - E_{1/2}^1$ ) and 0.24 V ( $\Delta E_{1/2}^2 = E_{1/2}^4 - E_{1/2}^3$ ),

respectively. Although the dimer system has strong complementary H-bonds and the peaks for the dimer can be preferentially observed in the NMR spectrum, the distance between the Re ions is 10.25 Å and there is no strong  $\pi$ -electron conjugation exists between the two Re ions because of the intervening H-bonds. Furthermore, when **1** is electrochemically oxidized at a constant potential (+0.28 V vs. Ag/AgCl) to generate the  $\text{Re}^{\text{III}}\text{Re}^{\text{IV}}$  species, no intervalence absorption band was observed, which supports the fact that there is no electronic interaction between the  $\text{Re}^{\text{III}}$  and  $\text{Re}^{\text{IV}}$  centers.<sup>[21]</sup> Why then are the mixed-valence states of  $\text{Re}^{\text{II}}\text{Re}^{\text{III}}$  and  $\text{Re}^{\text{III}}\text{Re}^{\text{IV}}$  stabilized? The two H-bonding protons connecting the two monomer units of the  $\text{Re}^{\text{III}}\text{Re}^{\text{III}}$  state of **1** would initially undergo the concerted double proton transfer through a symmetrical double-well potential surface with almost equivalent energies when both the  $\text{Re}^{\text{III}}$  centers are the same. When either of the  $\text{Re}^{\text{III}}$  centers is oxidized or reduced to the  $\text{Re}^{\text{IV}}$  or  $\text{Re}^{\text{II}}$  state, the symmetrical double-well potential surface is changed into an unsymmetrical one. Then, the two H-bonding protons would be localized to the site of the lower oxidation state of the Re units. Practically, the two mixed-valence states  $\text{Re}^{\text{II}}\text{Re}^{\text{III}}$  and  $\text{Re}^{\text{III}}\text{Re}^{\text{IV}}$  of **1** form the proton-transfer complexes  $[\{\text{Re}^{\text{II}}\text{Cl}_2(\text{L})(\text{H}_2\text{bim})\} \cdots \{\text{Re}^{\text{III}}\text{Cl}_2(\text{L}_2)(\text{bim})\}]^-$  and  $[\{\text{Re}^{\text{III}}\text{Cl}_2(\text{L}_2)(\text{H}_2\text{bim})\} \cdots \{\text{Re}^{\text{IV}}\text{Cl}_2(\text{L}_2)(\text{bim})\}]^+$ , respectively ( $\text{L} = \text{P}n\text{Bu}_3$ ). The lowest reduction wave and the highest oxidation wave correspond with the processes that yield  $[\{\text{Re}^{\text{II}}\text{Cl}_2(\text{L}_2)(\text{Hbim})\} \cdots \{\text{Re}^{\text{III}}\text{Cl}_2(\text{L}_2)(\text{Hbim})\}]^{2-}$  and  $[\{\text{Re}^{\text{IV}}\text{Cl}_2(\text{L}_2)(\text{Hbim})\} \cdots \{\text{Re}^{\text{IV}}\text{Cl}_2(\text{L}_2)(\text{Hbim})\}]^{2+}$ . In the former process only the deprotonated  $\{\text{Re}^{\text{III}}\text{Cl}_2(\text{L}_2)(\text{bim})\}^-$  unit in the dimer is reduced, and in the latter case only the protonated  $\{\text{Re}^{\text{III}}\text{Cl}_2(\text{L}_2)(\text{H}_2\text{bim})\}^+$  unit is oxidized. Thus, we considered that the reversibility of the redox waves of **1** is correlated to the proton-transfer motion. Therefore, to detect the rate-determining proton-transfer step in the redox reactions of **1**, the CV measurements were carried out in  $\text{CH}_2\text{Cl}_2$  at high velocities (up to  $10 \text{ V s}^{-1}$ ) and at low temperatures (ca.  $-60^\circ\text{C}$ ). A larger deviation in shapes of the redox waves of **1**, suggesting a chemical reaction attributed to the proton-migration process, was observed as a result of the influence of the slow proton transfer relative to the electron transfer. Such deviations in the separation of the oxidation and reduction peaks at high velocities and low temperatures have been observed for rate-determining proton-transfer processes in organic compounds.<sup>[22]</sup>

Theoretical calculations were performed by using DFT (B3LYP/6-31G\*\* and LANL2DZ) with Gaussian98<sup>[23]</sup> for two model complexes (the  $\text{Re}^{+3.5}\text{Re}^{+3.5}$  state  $[\{\text{Re}^{+3.5}\text{Cl}_2(\text{PH}_3)_2(\text{Hbim})\}_2]^+$  of **A** and the  $\text{Re}^{\text{III}}\text{Re}^{\text{IV}}$  state  $[\{\text{Re}^{\text{III}}\text{Cl}_2(\text{PH}_3)_2(\text{H}_2\text{bim})\} \cdots \{\text{Re}^{\text{IV}}\text{Cl}_2(\text{PH}_3)_2(\text{bim})\}]^+$  of **B** in Figure 4) to compare the stabilities of the mixed-valence states and to clarify the origin of the stabilization. It was assumed that the two H-bonding protons of model **A** are symmetrically distributed in both monomer units and that the positive charge on each Re ion is equivalent to an oxidation state of +3.5. In contrast, the two H-bonding protons in model **B** are localized on the side of the  $\text{Re}^{\text{III}}$  unit and the positive charge is present on the side of the  $\text{Re}^{\text{IV}}$  unit. As a result, the potential energy of the mixed-valence state of **1** is described as a



**Figure 4.** Two proton-transfer models of  $[\{\text{ReCl}_2(\text{PH}_3)_2(\text{Hbim})\}]_2$  used in the calculations.

double-well curve, and model **B** is relatively more stable than model **A** by  $3.96 \text{ kcal mol}^{-1}$  (Figure 5 and Table 1). In model **B**, a unit of  $\{\text{Re}^{\text{III}}\text{Cl}_2(\text{PH}_3)_2(\text{H}_2\text{bim})\}^+$  in the dimer has a charge

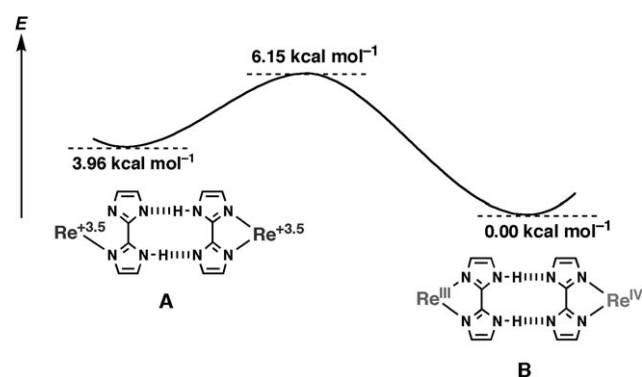


**Figure 5.** Calculation results for models **A** and **B**.

**Table 1:** Calculated values of charges and spin densities of each monomer fragment (SD) and Re ion (SD-Re) in models **A** and **B**.

| Model  | Left fragment |      |       | Right fragment |      |       |
|--|---------------|------|-------|----------------|------|-------|
|  | Charge        | SD   | SD-Re | Charge         | SD   | SD-Re |
| $\text{Re}^{\text{III}}\text{Re}^{\text{III}}$ |               |      |       |                |      |       |
| <b>A</b>                                       | 0.000         | 2.00 | 1.78  | 0.000          | 2.00 | 1.78  |
| <b>B</b>                                       | 0.595         | 2.00 | 1.79  | -0.595         | 2.00 | 1.79  |
| $\text{Re}^{\text{III}}\text{Re}^{\text{IV}}$  |               |      |       |                |      |       |
| <b>A</b>                                       | 0.500         | 2.50 | 2.12  | 0.500          | 2.50 | 2.12  |
| <b>B</b>                                       | 0.764         | 2.00 | 1.79  | 0.236          | 3.00 | 2.38  |
| $\text{Re}^{\text{IV}}\text{Re}^{\text{IV}}$   |               |      |       |                |      |       |
| <b>A</b>                                       | 1.000         | 3.00 | 2.44  | 1.000          | 3.00 | 2.44  |
| <b>B</b>                                       | 1.619         | 3.00 | 2.46  | 0.381          | 3.00 | 2.43  |

of  $+0.764$  and the other unit  $\{\text{Re}^{\text{IV}}\text{Cl}_2(\text{PH}_3)_2(\text{bim})\}$  has a charge of  $+0.236$ . Thus, according to the proton transfer from **A** to **B** over an energy barrier of  $6.15 \text{ kcal mol}^{-1}$ , a proton leaves from an N–H group, leaving an electron pair on the N atom, and connects with the lone-pair electrons of the opposite N atom to form a new N–H bond. Therefore, the stabilization of model **B** with an unsymmetrical double-well

potential energy surface is very important for proton transfer, because the symmetrical double-well potential does not provide any driving force for this transfer. Further, calculations for models with equivalent charges  $\text{Re}^{\text{III}}\text{Re}^{\text{III}}$  and  $\text{Re}^{\text{IV}}\text{Re}^{\text{IV}}$  revealed energy curves for proton transfer that are nearly a single well. Furthermore, the two protons are not distributed on one biimidazole ligand in these models (see Figure 4S in the Supporting Information). Further stabilization is expected when outer-sphere solvent reorganization is considered in the calculation.

In conclusion, dimer **1** is formed preferentially over the corresponding monomers in nonaqueous solvents, such as toluene and  $\text{CH}_2\text{Cl}_2$ . CV measurements show that **1** reversibly generates stable mixed-valence states  $\text{Re}^{\text{III}}\text{Re}^{\text{IV}}$  upon oxidation and  $\text{Re}^{\text{II}}\text{Re}^{\text{III}}$  upon reduction. There are no intervalence absorption bands for the  $\text{Re}^{\text{III}}\text{Re}^{\text{IV}}$  state. As a result, it is reasonable that the mixed-valence states are stabilized by proton transfer of the complementary H-bonds; evidently, this proton transfer is unique and probably different from that demonstrated previously by Hammes-Schiffer and Mayer and co-workers, because the solvent molecules do not participate in the reactions. Theoretical calculations support the formation of the  $\text{Re}^{\text{III}}\text{Re}^{\text{IV}}$  state (rather than  $\text{Re}^{3.5}\text{Re}^{3.5}$ ) upon one-electron oxidation of **1**. The proton-transfer mechanisms of this system are a matter for further investigation.

## Experimental Section

**Synthesis of 2:**  $\text{PnBu}_3$  (4.3 mL, 16.7 mmol) in  $\text{Et}_2\text{O}$  was added to a solution of  $[\text{Re}^{\text{III}}\text{Cl}_2(\text{PPh}_3)_2(\text{H}_2\text{bim})]\text{Cl}$  (2.10 g, 2.21 mmol) in benzene (100 mL), and the mixture was refluxed for 6 h. The obtained solution was evaporated to dryness, and the residue was recrystallized from  $\text{Et}_2\text{O}$ /hexane to give orange crystals. Yield: 1.20 g (65.3 %).

**Synthesis of 1:**  $\text{NH}_3$  gas was slowly diffused through a solution of **2** (0.10 g, 0.12 mmol) in MeOH (5  $\text{cm}^3$ ), and red crystals were obtained. Yield: 0.80 g (41.8 %). Detail of the characterization are given in the Supporting Information.

Received: March 23, 2007

Published online: July 5, 2007

**Keywords:** coordination chemistry · electron transfer · hydrogen bonds · proton transfer · supramolecular chemistry

- a) M. Y. Okamura, G. Feher, *Annu. Rev. Biochem.* **1992**, *61*, 861; b) P. J. P. Williams, *Nature* **1995**, *376*, 643; c) S. Iwata, C. Ostermelter, B. Ludwig, H. Michel, *Nature* **1995**, *376*, 660.
- a) B. Albert, D. Bray, A. Johnson, J. Lewis, M. Raff, K. Roberts, P. Walter, *Molecular Biology of the Cell*, Garland, New York, **1994**; b) L. Stryer, *Biochemistry*, Freeman, New York, **1995**.
- a) T. Mitani, T. Inabe, *Advances in spectroscopy*, Vol. 22 (Eds.: R. J. H. Clark, R. E. Hester), Wiley, New York, **1993**, p. 291; b) T. Mitani, G. Saito, H. Urayama, *Phys. Rev. Lett.* **1988**, *60*, 2299.
- a) W. W. Cleland, M. M. Kreevoy, *Science* **1994**, *264*, 1887; b) J. Lin, W. M. Westler, W. W. Cleland, J. L. Markley, P. A. Frey, *Proc. Natl. Acad. Sci. USA* **1998**, *95*, 14664.
- H. Terao, T. Sugawara, Y. Kita, N. Sato, K. Eriko, S. Takeda, *J. Am. Chem. Soc.* **2001**, *123*, 10468–10474.
- K. Nakasuji, T. Kitagawa, K. Okaniwa, T. Mitani, *J. Am. Chem. Soc.* **1991**, *113*, 1862–1864.

- [7] T. Akutagawa, S. Takeda, T. Hasegawa, T. Nakamura, *J. Am. Chem. Soc.* **2004**, *126*, 291–294.
- [8] T. Mitani, H. Kitagawa, *Electrical and related properties of organic solids*, Kluwer Academic, Dordrecht, **1997**, p. 12 (NATO ASI Series, Vol. 24).
- [9] T. Akutagawa, T. Hasegawa, T. Nakamura, T. Inabe, G. Saito, *Chem. Eur. J.* **2002**, *8*, 4402–4411.
- [10] S. Hammes-Schiffer, *Acc. Chem. Res.* **2001**, *34*, 273–281; S. Hammes-Schiffer, *ChemPhysChem* **2002**, *3*, 33–42.
- [11] J. P. Roth, S. Lovel, J. M. Mayer, *J. Am. Chem. Soc.* **2000**, *122*, 5486.
- [12] A. M. Bond, M. Haga, *Inorg. Chem.* **1986**, *25*, 4507–4514.
- [13] P. Gilli, V. Bertolasi, V. Ferretti, G. Gilli, *J. Am. Chem. Soc.* **1994**, *116*, 909–915.
- [14] L. Leiserowitz, *Acta Crystallogr. Sect. B* **1976**, *32*, 775.
- [15] S. Nagaoka, T. Terao, F. Imashiro, A. Saika, N. Hirota, S. Hayashi, *J. Chem. Phys.* **1983**, *79*, 4694; B. H. Meier, F. Graf, R. R. Ernst, *J. Chem. Phys.* **1982**, *76*, 767; J. L. Skinner, H. P. Trommsdorff, *J. Chem. Phys.* **1988**, *89*, 897.
- [16] J. A. S. Smith, B. Wehrle, F. A. Parrilla, H.-H. Limbach, M. de la Concepción Foces-Foces, F. H. Cano, J. Elguero, A. Baldy, M. Pierrot, M. M. T. Khurshid, J. B. Larcombe-MacDouall, *J. Am. Chem. Soc.* **1989**, *111*, 7304–7312.
- [17] a) H. Mori, E. Miyoshi, *Bull. Chem. Soc. Jpn.* **2004**, *77*, 687–690; b) H. Mori, E. Miyoshi, *Chem. Lett.* **2004**, *33*, 758–759.
- [18] S. Fortin, P.-L. Fabre, M. Dartiguenave, A. L. Beauchamp, *J. Chem. Soc. Dalton Trans.* **2001**, 3520–3527.
- [19] Crystal data for **1**:  $[\{\text{ReCl}_2(\text{PnBu}_3)_2(\text{Hbim})\}]_2$ ,  $\text{C}_{30}\text{H}_{59}\text{Cl}_2\text{N}_4\text{P}_2\text{Re}$ ,  $M_r = 794.89$ , monoclinic, space group  $P2_1/c$  (No. 14),  $a = 11.830(1)$ ,  $b = 18.730(2)$ ,  $c = 16.880(2)$  Å,  $\beta = 96.700(2)^\circ$ ,  $V = 3714.7(7)$  Å<sup>3</sup>,  $Z = 4$ ,  $T = -100^\circ\text{C}$ ,  $R_1 = 0.028$  and  $R_w = 0.038$  ( $I > 3.00\sigma(I)$ ) and GOF = 0.776. CCDC-640909 contains the supplementary crystallographic data for this paper. These data can be obtained free of charge from The Cambridge Crystallographic Data Centre via [www.ccdc.cam.ac.uk/data\\_request/cif](http://www.ccdc.cam.ac.uk/data_request/cif).
- [20] a) W. C. Hamilton, J. A. Ibers, *In Hydrogen Bonding in Solid* (Eds.: R. Breslow, M. Karplus), Benjamin, New York, **1968**; b) G. C. Pimentel, A. L. MacClellan, *The Hydrogen Bond* (Ed.: L. Pauling), Reinhold, New York, **1960**.
- [21] a) C. Creutz, *Prog. Inorg. Chem.* **1983**, *30*, 1–73; b) C. Creutz, H. Taube, *J. Am. Chem. Soc.* **1973**, *95*, 1086.
- [22] F. Thomas, O. Jarjayes, H. Jamet, S. Hamman, E. S. Aman, C. Duboc, J.-L. Pierre, *Angew. Chem.* **2004**, *116*, 604–607; *Angew. Chem. Int. Ed.* **2004**, *43*, 594–597.
- [23] Gaussian 98 (Revision A.9): M. J. Frisch et al., see the Supporting Information.